Oncogene (2008) 27, 4592–4602
© 2008 Macmillan Publishers Limited All rights reserved 0950-9232/08 $30.00
www.nature.com/onc

ORIGINAL ARTICLE

Array CGH demonstrates characteristic aberration signatures in human papillary thyroid carcinomas governed by RET/PTC

K Unger[1,2,9], E Malisch[1,9], G Thomas[2], H Braselmann[1], A Walch[3], G Jackl[4], P Lewis[5], E Lengfelder[6], T Bogdanova[7], J Wienberg[8] and H Zitzelsberger[1]

[1]*Institut für Molekulare Strahlenbiologie, Helmholtz Zentrum München—Deutsches Forschungszentrum für Gesundheit und Umwelt GmbH, Germany;* [2]*Department of Histopathology, Hammersmith Hospital, London, UK;* [3]*Institut für Pathologie, Helmholtz Zentrum München—Deutsches Forschungszentrum für Gesundheit und Umwelt GmbH, Germany;* [4]*Institut für Strahlenbiologie, Helmholtz Zentrum München—Deutsches Forschungszentrum für Gesundheit und Umwelt GmbH, Germany;* [5]*Swansea Medical School, Swansea University, Singleton Park, Swansea, UK;* [6]*Strahlenbiologisches Institut, Ludwig Maximilians Universität, München, Germany;* [7]*Institute of Endocrinology and Metabolism, Academy of Medical Sciences of the Ukraine, Kiev, Ukraine and* [8]*Department Biologie II, Anthropologie und Humangenetik, Ludwig Maximilians Universität, München, Germany*

The aim of this study is to investigate additional genetic alterations in papillary thyroid carcinomas (PTCs) with known RET/PTC rearrangements. We applied array-based comparative genomic hybridization (array CGH) to 33 PTC (20 PTC from adults, 13 post-Chernobyl PTC from children) with known RET/PTC status. Principal component analysis and hierarchical cluster analysis identified cases with similar aberration patterns. Significant deviations between tumour-groups were obtained by statistical testing (Fisher's exact test in combination with Benjamini–Hochberg FDR-controlling procedure). FISH analysis on FFPE sections was applied to validate the array CGH data. Deletions were found more frequently in RET/PTC-positive and RET/PTC-negative tumours than amplifications. Specific aberration signatures were identified that discriminated between RET/PTC-positive and RET/PTC-negative cases (aberrations on chromosomes 1p, 3q, 4p, 7p, 9p/q, 10q, 12q, 13q and 21q). In addition, childhood and adult RET/PTC-positive cases differ significantly for a deletion on the distal part of chromosome 1p. There are additional alterations in RET/PTC-positive tumours, which may act as modifiers of RET activation. In contrast, alterations in RET/PTC-negative tumours indicate alternative routes of tumour development. The data presented serve as a starting point for further studies on gene expression and function of genes identified in this study.
Oncogene (2008) **27,** 4592–4602; doi:10.1038/onc.2008.99; published online 14 April 2008

Keywords: papillary thyroid carcinoma; array CGH; RET/PTC; candidate genes; tumour development; aberration signature

Correspondence: Dr H Zitzelsberger, Helmholtz Zentrum München, Institute for Molecular Radiobiology, Ingolstädter-Landstraße 1, Neuherberg D-85764, Germany.
E-mail: zitzelsberger@helmholtz-muenchen.de
[9]These authors contributed equally to this study.
Received 19 July 2007; revised 29 November 2007; accepted 29 February 2008; published online 14 April 2008

Introduction

A frequent genetic alteration in papillary thyroid carcinomas (PTCs) is rearrangement of the *RET* proto-oncogene, which has been assigned to chromosomal band 10q11.2 (Grieco *et al*., 1990; Pierotti *et al*., 1992). RET/PTC oncogenic activation is the result of chromosomal rearrangements, which fuse the RET tyrosine kinase (RET-TK) domain to the 5′-terminal region of heterologous genes. The rearrangements are a marker for PTCs as their very name RET/*PTC* implies. At least 16 chimeric mRNAs involving 11 different genes have been reported (reviewed in Santoro *et al*., 2004) of which RET/PTC1 (RET rearrangement with H4) and RET/PTC3 (RET rearrangement with RFG/ELE1) are by far the most common (Santoro *et al*., 2004). The incidence of RET/PTC in radiation-induced childhood PTCs is in the range of 50–70% (Klugbauer *et al*., 1995; Smida *et al*., 1999; Thomas *et al*., 1999; Rabes *et al*., 2000), whereas in sporadic papillary carcinomas in adults the incidence is somewhat lower (5–30%) (Jhiang and Mazzaferri, 1994). However, the identification of RET/PTC in other common thyroid tumour histotypes such as oncocytic adenomas and carcinomas (Cheung *et al*., 2000), and even in hyperplastic thyroid nodules (Ishizaka *et al*., 1991; Elisei *et al*., 2001) and Hashimoto's thyroiditis (Rhoden *et al*., 2006), seems to challenge the validity of RET/PTC as a tumour marker and its specificity for PTC. Moreover, it has been recently shown that the level of RET/PTC expression in papillary carcinoma is highly variable, suggesting that the distribution of RET/PTC within one tumour may not be homogenous (Rhoden *et al*., 2004; Unger *et al*., 2004). This is also supported by recent fluorescence *in situ* hybridization (FISH) studies by ourselves and others (Unger *et al*., 2004; Ciampi and Nikiforov, 2007).

To investigate whether other genes are involved in thyroid carcinogenesis, we have studied a series of PTCs by array-based comparative genomic hybridization (array CGH). Array CGH represents an approach using mapped sequences arrayed onto glass slides instead of

metaphase chromosomes that are used in conventional CGH as hybridization targets. This generates a higher resolution dependent on the insert size and density of the mapped sequences. In this study, we used bacterial artificial chromosome (BAC)-arrays (~3400 clones) that allow the examination of the entire genome for chromosomal copy number changes (DNA gains and losses) with a resolution of 1 Mb. A striking advantage of this technology is its use on archival paraffin-embedded material (van Beers *et al*., 2006).

In this study on PTC, array CGH was used to investigate chromosomal changes in 33 papillary thyroid post-Chernobyl adult and childhood PTC. In all cases, the tumours have been pre-characterized in terms of RET/PTC rearrangements.

The aim of this study was to determine differences in chromosomal aberration patterns between RET/PTC-positive and -negative PTC. The identification of characteristic alteration signatures in different tumour groups (adult, childhood, RET/PTC-positive, RET/PTC-negative) enabled a subsequent characterization of candidate genes that may either cooperate with or substitute for RET/PTC in papillary thyroid carcinogenesis.

Results

We analysed 33 post-Chernobyl PTCs from adults and children for chromosomal changes by array CGH. The tumours were also characterized for the presence of RET/PTC rearrangements on a single-cell level by FISH. The RET/PTC status of each tumour and the patient's demographic and clinical data are summarized in Table 1.

Chromosomal imbalances, hierarchical cluster analysis and principal component analysis

In general, DNA losses occurred more frequently than DNA gains. The most frequent imbalances (in more than 30% of tumours) were losses on chromosomes 1, 6, 7, 9, 10, 11, 12, 13, 16, 19, 20, 22 and gains on chromosomes 10, 12, 19, 20, 21 (Figure 1). Hierarchical cluster analysis (HCA) employing the correlations between the array CGH profiles segregated significantly nine adult RET/PTC-negative cases from all other cases (Fisher's exact test, $P<0.05$; Figure 2). The patterns of array CGH differences observed using HCA were confirmed using principal component analysis

Table 1 Patient data and RET/PTC status

Case no.	*Gender/age (years)*	*Histology*	*Histological variant*	*RET/PTC status*[a]	*BRAF T1796A mutation*[b]
1	F/35	PTC, pT4aN1aM0	Papillary	RET/PTC1	+
2	F/32	PTC, pT4bN1aM0	Follicular	RET/PTC1	−
3	M/32	PTC, pT4aN1aM0	Papillary	RET/PTC1	−
4	F/42	PTC, pT4bN1aM0	Mixed	RET/PTC3	−
5	F/37	PTC, pT4aN1aM0	Papillary	RET/PTC1	−
6	M/31	PTC, pT4bN1M0	Papillary	RET/PTC3	−
7	M/21	PTC, pT4bN1bM0	Papillary	RET/PTC3	−
8	F/26	PTC, pT4bN1bM0	Papillary	RET/PTC3	−
9	F/28	PTC, pT4bN2bM0	Papillary	RET/PTC-positive	−
10	F/36	PTC, pT4N1bM0	Solid	RET/PTC1	−
11	F/35	PTC, pT4bN0M0	Papillary	RET/PTC-negative	−
12	F/32	PTC, pT2aN0M0	Solid	RET/PTC-positive	−
13	F/32	PTC, pT3N0M0	Papillary	RET/PTC-negative	−
14	F/42	PTC, pT4aN1aM0	Papillary	RET/PTC-negative	+
15	F/37	PTC, pT4bN1bM0	Papillary	RET/PTC-negative	−
16	F/31	PTC, pT4aN1bM0	Papillary	RET/PTC-negative	−
17	F/21	PTC, pT4aN1bM0	Papillary	RET/PTC-negative	+
18	M/26	PTC, pT3aN1aM0	Papillary	RET/PTC-negative	−
19	F/28	PTC, pT4aN1aM0	Papillary	RET/PTC-negative	−
20	F/36	PTC, pT4aN1aM0	Papillary	RET/PTC-negative	−
21	M/8	PTC, pT4N2M0	Follicular-solid	RET/PTC3	−
22	M/10	PTC, pT4N2M1	Follicular-solid	RET/PTC1	−
23	F/15	PTC, pT4N2M0	Follicular-solid	RET/PTC3	−
24	F/11	PTC, pT4N2M1	Follicular-solid	RET/PTC1	−
25	F/15	PTC, pT4N2M1	Follicular-solid	RET/PTC3	−
26	F/14	PTC, pT4N2M1	Follicular-solid	RET/PTC3	−
27	F/11	PTC, pT4N1b,M0	Solid	RET/PTC3	−
28	M/13	PTC, pT4N2M1	Follicular-solid	RET/PTC-negative	−
29	M/10	PTC, pT4N1M0	Follicular-solid	RET/PTC-negative	−
30	F/14	PTC, pT4N0M0	Follicular-solid	RET/PTC-positive	−
31	F/10	PTC, pT4N1M1	Follicular-solid	RET/PTC-negative	−
32	F/10	PTC, pT4N1M1	Follicular-solid	RET/PTC-positive	−
33	M/10	PTC, pT4N0M0	Follicular-solid	RET/PTC-positive	−

Abbreviations: F, female; M, male; RET/PTC-negative, no indication for elevated RET tyrosine kinase (TK) expression or specific RET rearrangement; RET/PTC-positive, elevated expression of TK domain in comparison to extracellular domain, measured by reverse transcription–PCR; PTC, papillary thyroid carcinoma; +, mutation present; −, mutation absent.
[a]As previously published in Smida *et al*., 1999 and Unger *et al*., 2006.
[b]BRAF mutation analysed according to Powell *et al*., 2005.

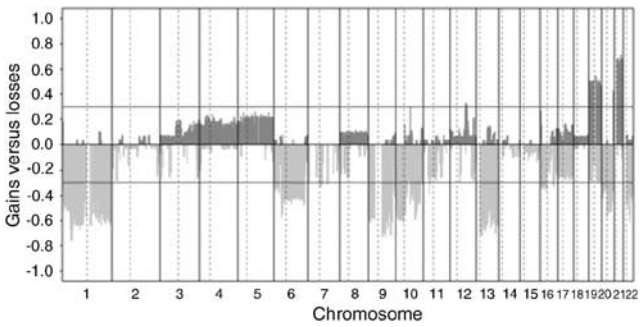

Figure 1 Frequencies (1.0 = 100%) of gains (red) and losses (green) in 33 papillary thyroid carcinomas. Horizontal line marks 30% frequency.

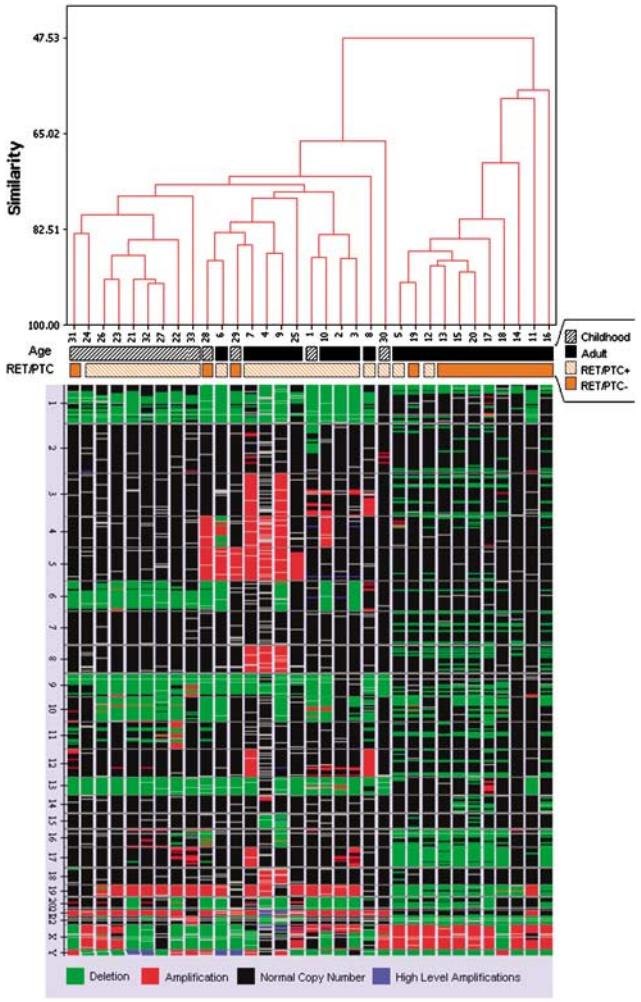

Figure 2 Dendrogram of hierarchical cluster analysis based on average linkage and correlation coefficient distance. Coloured bars indicate adult (black), childhood (grey), RET/PTC-positive (orange-hatched) and RET/PTC-negative (orange) cases. DNA gains (red) and losses (green) are arranged by tumour groups. High-level amplifications are indicated in blue.

(Supplementary Figure 1 is available at the following website: http://cancerinformatics.swansea.ac.uk/path/thyroidcgh.aspx).

Comparison of tumour groups

On the basis of the results from the cluster analysis, we grouped tumours into RET/PTC-positive from adults, RET/PTC-positive from children and RET/PTC-negative tumours from adults and analysed them for significant differences. Chromosomal imbalances arranged by each tumour group are visualized by frequency plots (Figure 3). As deviations between these frequency plots were visible, each BAC clone was examined for the difference between two tumour groups by the Fisher's exact test. Significant test results (adjusted P-value <0.05) were obtained for adult RET/PTC-positive versus adult RET/PTC-negative cases (1253 BAC clones were tested, 441 were significant on different chromosomes) and for adult RET/PTC-positive versus childhood RET/PTC-positive cases (1239 BAC clones were tested, 34 were significant, all on chromosome 1p35.3–36.31). Significant differences are summarized in Table 2. The majority of these aberrations are specific for RET/PTC-positive cases. Characteristic aberration signatures became apparent discriminating between RET/PTC-positive and RET/PTC-negative cases (aberrations on chromosome 1p, 3q, 4p, 7p, 9p/q, 10q, 12q, 13q and 21q). In addition, childhood and adult RET/PTC-positive cases differ significantly for a deletion on the distal part of chromosome 1p.

FISH analysis and candidate genes

Amplified and deleted regions from array CGH analysis were confirmed by FISH on formalin-fixed and paraffin-embedded (FFPE) sections using digoxigenin or biotin-labelled BAC clones (Figure 4). All chromosomal imbalances with exception of deletion 1q31 in cases 27 and 28 and deletion 1p22 in case 28 were validated. The frequency of aberrant FISH signals in each case investigated is given in Table 3.

For chromosomal regions that showed significant differences in two tumour groups or consistency in all tumour groups, candidate genes have been selected from the Ensembl database (www.ensembl.org). Specific candidates that have been reported to be related to tumour growth and development are highlighted in Tables 4 and 5.

Examples of an altered consensus region on 1p36.31–35.3 (deletion), 7q21.3–22.1 (deletion) and 12q24.23–24.31 (amplification) as well as confirmatory FISH analyses on a FFPE sections are shown in Figure 4.

Involvement of candidate genes in molecular pathways

We identified 31 cancer-related candidate genes. For the retrieval of pathways linking these candidate genes, we used the web-accessible Pathway Interaction Database (National Cancer Institute, http://www.pid.nci.nih.giv). This database search revealed a subset of candidate genes (Jak1, Jak2, Tnf, Pten, Foxo1A, Rb1 and Tiam1) that exhibit molecular interactions and could be linked to the apoptosis, interleukin-27, angiopoietin receptor and the phosphatidyl-inositol 3-kinase (PI3K)/mitogen-activated protein (MAP) kinase pathways.

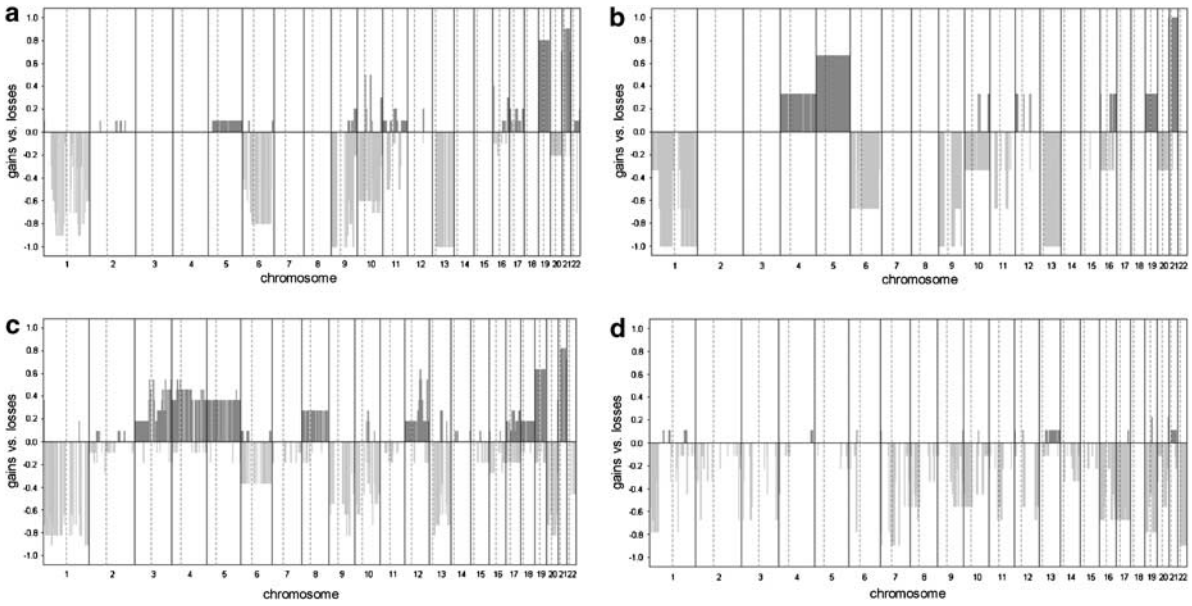

Figure 3 Frequencies (1.0 = 100%) of gains (red) and losses (green) in four groups of papillary thyroid carcinoma (PTC): RET/PTC-positive post-Chernobyl tumours from children (**a**), RET/PTC-negative post-Chernobyl tumours from children (**b**), RET/PTC-positive tumours from adults (**c**), RET/PTC-negative tumours from adults (**d**).

Table 2 Characteristic aberrations in RET/PTC-positive and RET/PTC-negative PTCs

Chromosome	*Chromosomal region*	*Region start (BAC)*	*Region end (BAC)*	*Size (Mb)*	*Number of annotated proteins*[a]	*Characteristic for tumour group*
Gains						
3	p12.2–13.1	RP11-510B7	RP11-40M23	24.74	60	RET/PTC-positive[b]
3	q26.1	RP11-491K7	RP11-12N13	0.61	1	RET/PTC-positive[b]
3	q29	RP11-279P10	RP11-252K11	1.91	18	RET/PTC-positive[b]
4	p14–q13.1	RP11-20M7	RP11-24H13	2.46	81	RET/PTC-positive[b]
12	q21.2–21.33	RP11-26L7	RP11-239F20	13.57	36	RET/PTC-positive[b]
12	q24.23–24.31	RP11-144B2	RP11-44F24	1.38	31	RET/PTC-positive[b]
19	pter–qter	CTD-3113P16	GS1-1129C9	63.59	1315	RET/PTC-positive[b]
21	q11.2–qter	RP11-193B6	CTB-63H24	33.47	222	RET/PTC-positive[b]
Losses						
1	p36.31–35.3	RP11-49J3	RP4-783C10	32.15	411	Adults[c]
1	p33–cen	RP11-330M19	RP11-418J17	71.68	389	RET/PTC-positive[b]
1	q23.2–32.1	RP11-190A12	RP11-469A15	40.72	249	RET/PTC-positive[b]
1	q32.2–qter	RP11-564A8	CTB-160H23	42.09	277	RET/PTC-positive[b]
7	p22.2–p22.1	RP11-348A21	RP1-42M2	2.54	12	RET/PTC-negative[d]
7	p11.2—q11.23	RP4-725G10	RP11-107L23	19.04	64	RET/PTC-negative[d]
7	q21.3–22.1	RP11-380G21	RP11-333G13	4.05	82	RET/PTC-negative[d]
9	pter–p21.1	GS1-41L13	RP11-48L13	29.64	11	RET/PTC-positive[b]
9	q31.1	RP11-96L7	RP11-318L4	4.49	2	RET/PTC-positive[b]
9	p23–q33.2	RP11-534I8	RP11-360A18	110.36	105	RET/PTC-positive[b]
10	q23.2–23.32	RP11-470J18	RP11-92H8	6.83	42	RET/PTC-positive[b]
10	q25.1	RP11-165P9	RP11-478K18	2.66	1	RET/PTC-positive[b]
13	q12.11–21.2	RP11-309H15	RP11-245B11	40.9	175	RET/PTC-positive[b]
13	q22.1–34	RP11-76K19	RP11-359P14	95.07	60	RET/PTC-positive[b]
20	p12.3–12.1	RP5-959I16	RP5-822J19	9.38	21	RET/PTC-positive[b]

Abbreviations: FDR, false discovery rate; PTC, papillary thyroid carcinoma. [a]According to www.ensembl.org. [b]Comparison between RET/PTC-positive and RET/PTC-negative adults, Fisher's exact test, $P<0.017$, corresponding to FDR = 0.05. [c]Comparison between RET/PTC-positive adults and children, Fisher's exact test, $P<0.0011$, corresponding to FDR = 0.05. [d]Comparison between RET/PTC-positive and RET/PTC-negative adults, Fisher's exact test, $P<0.017$, corresponding to FDR = 0.05.

Genetic heterogeneity in RET/PTC-positive case no. 3
Three histologically similar areas in PTC case no. 3, as well as the whole tumour have been analysed by array CGH. Recurrent regions of chromosomal imbalances in all four samples were deletions on 1p34.1–13 (109.4 Mb), 1q12–21 (28.7 Mb), 1q22–44 (92.5 Mb),

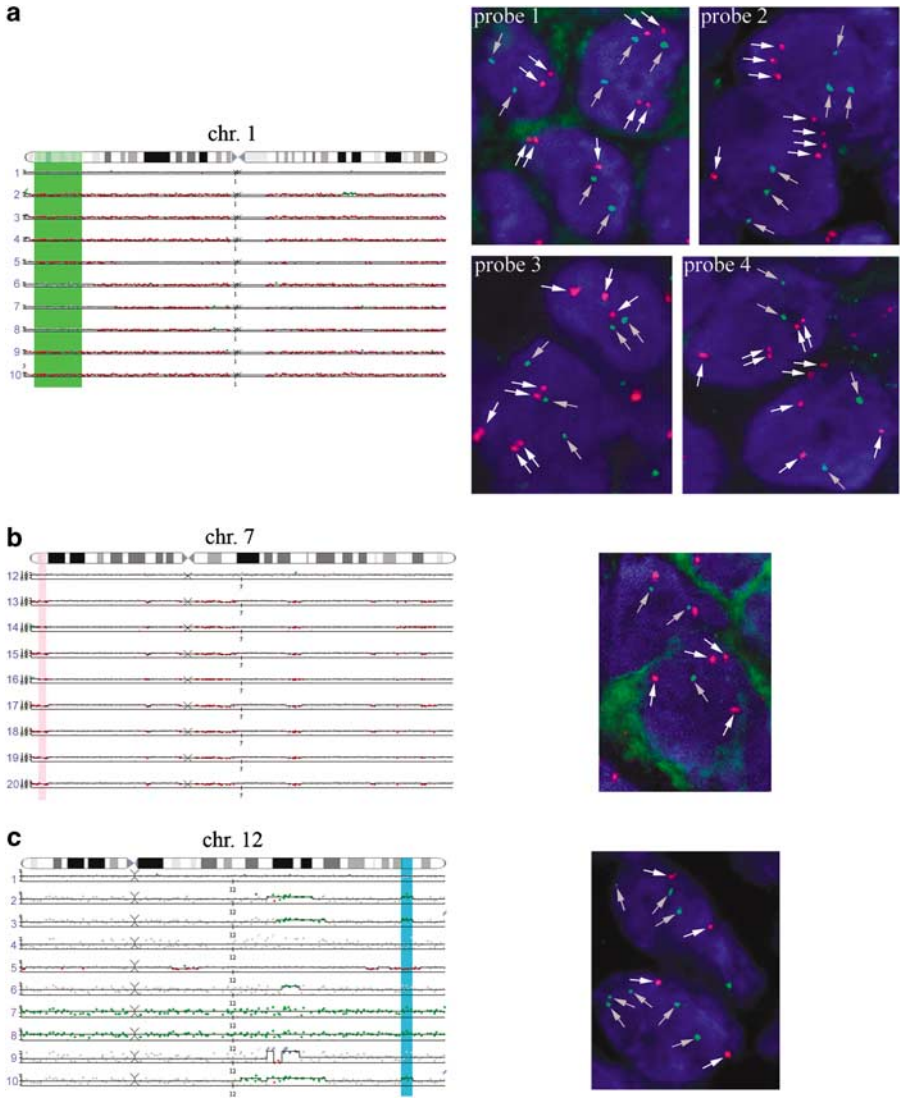

Figure 4 Array comparative genomic hybridization (CGH) and fluorescence *in situ* hybridization (FISH) evaluation from papillary thyroid carcinoma (PTC) with a deletion on chromosome 1p35.3–36.31, a deletion on 7q21–22 and an amplification on 12q24. (**a**) The panel on the left shows array CGH profiles of chromosome 1 from cases 1 to 10 (adult, RET/PTC positive). Each dot represents the log2 ratio of a bacterial artificial chromosome (BAC) clone (grey: no alteration; red: deletion; green: amplification). The deletion (1p35.3–36.31) specific for the adult RET/PTC-positive cases is indicated by a green bar. The right panel shows confirmatory FISH analysis of cases harbouring the 1p35.3–36.31 deletion using BAC clones RP11-49J3 (FISH probe 1) on case no. 10, RP4-783C10 (FISH probe 2) on case no. 1, RP11-719E21 (FISH probe 3) on case no. 3 and RP11-58A11 (FISH probe 4) on case no. 2, each in combination with a reference BAC clone (RP11-136K15). Region-specific FISH signals (green) are indicated by grey and reference FISH signals (red) by white arrows. Cells with a deletion on 1p35.3–36.31 show fewer region-specific FISH signals than reference FISH signals. (**b**) Array CGH profiles of chromosome 7 (left) displaying a minimal region of deletion on 7q21–22 (high lightened by a pink bar). The image to the right shows hybridization of pooled BACs RP11-442P13 and RP11-152I5 specific for 7p22.1 (green FISH signals, grey arrows) and of reference clone RP11-328M22 (red FISH signals, white arrows) on tumour case no. 16. A tetraploid cell harbouring the deletion 7p22.1 shows four red FISH signals and only one green signal. The neighbouring cell is diploid with two red and green FISH signals each (**c**) Array CGH profiles (left) of chromosome 12 displaying a minimal region of amplification on 12q24 (highlightened by a blue-green bar). Pooled BAC clones RP11-15J22 and RP11-18E11 (green FISH signals, grey arrows) and pooled reference BAC clones RP11-572H20 and RP11-109F12 (red FISH signals, white arrows) were hybridized on paraffin sections of case no. 10 to confirm the amplification on 12q24 identified by array CGH. Two diploid cells with amplified green FISH signals are shown to the right.

13q12–34 (94.6 Mb) and amplifications on 19p13.3–13.4 (63.4 Mb), 20q13.3 (0.9 Mb), 21q11.2–22 (33.3 Mb). All microdissected areas showed additional imbalances (Figure 5), indicating a distinct genetic heterogeneity within different areas of the same PTC.

Discussion

We describe distinct chromosomal changes in PTCs identified by array CGH. To our knowledge, this represents the first array CGH study on PTCs, which includes post-Chernobyl thyroid tumours. We report

Table 3 Interphase FISH analysis with BAC clones for confirmation of array CGH results

Case no.	*Aberration by array CGH*	*BAC clone tested*	*Frequency of cells with normal FISH signals (%)*[a]	*Frequency of cells with aberrant FISH signals (%)*[a]
1	amp 3p12	RP11-104L22	48.6	51.4
1	amp 12q24	RP11-18E11	50.8	49.2
2	amp 13q21	RP11-89G11	50.5	49.5
2	amp 20q13	RP11-358D14	45.5	54.5
3	amp 3p12	RP11-104L22	51.5	48.5
3	amp 12q24	RP11-18E11	51.8	48.2
10	del 1p35.3–36.31	RP11-49J3	31.0	69.0
10	amp 13q21	RP11-89G11	56.2	43.8
10	amp 20q13	RP11-358D14	47.7	52.3
13	del 7p22	RP11-442P13	47.7[b]	52.3[b]
13	del 19q13	RP11-537N4	48.9[c]	51.1[c]
15	del 19q13	RP11-537N4	42.9[c]	57.2[c]
17	del 7p22	RP11-442P13	43.7[b]	56.3[b]
22	del 6q21	RP11-654F13	54.2[d]	45.8[d]
26	del 1q31	RP11-48A18	100[e]	0[e]
26	del 1p22	RP11-504G14	55.2[f]	44.8[f]
27	del 1q31	RP11-48A18	100[e]	0[e]
27	del 1p22	RP11-504G14	100[f]	0[f]
28	del 6q21	RP-654F13	60.1[d]	39.9[d]

Abbreviations: BAC, bacterial artificial chromosome; CGH, comparative genomic hybridization; FISH, fluorescence *in situ* hybridization.
[a]At least 100 interphase nuclei scored.
[b]Co-hybridization with clone RP11-328M22 (7q31) for reference.
[c]Co-hybridization with clone CTD-2043I16 (19q12) for reference.
[d]Co-hybridization with clone RP3-349A12 (6p21) for reference.
[e]Co-hybridization with clone RP4-663N10 (1cen) for reference.
[f]Co-hybridization with clone RP4-663N10 (1cen) for reference.

Table 4 Tumour-related candidate genes identified in regions specific for RET/PTC-positive (+) or RET/PTC-negative cases (−)

Chromosomal region	*Candidate genes*	*Type of aberration*	*Characteristic for tumour group*
1p33–cen	RAB3B, JAK1, TGFBR3	Deletion	+
1p35.3–36.31	TNFRSF25, CASP9	Deletion	+ (adults)
3q29	MUC4, PPP1R2, TFRC	Amplification	+
7p22.1	RBAK	Deletion	−
4p14–13.1	RHOH	Amplification	+
9p21.2–24.3	JAK2, TUSC1	Deletion	+
9q22.33–31.1	STX17	Deletion	+
9q32–33.1	TNFSF15, DEC1, DBC1	Deletion	+
10q23.2–23.32	PTENP1, PTEN	Deletion	+
12q24.23–24.31	CAMKK2, PXN, RNF34	Amplification	+
13q12.11–21.2	LATS2, RASL11A, FOXO1A, RB1, DLEU7	Deletion	+
13q22.1–34	SLITRK1, SLITRK5, SLITRK6, ING1	Deletion	+
21q21.3–22.3	TIAM1, ERG	Amplification	+

Table 5 Tumour-related candidate genes identified in recurrent regions of all three thyroid tumour subgroups

Chromosomal region	*Candidate genes*	*Type of aberration*
9q21.33	RMI1, GAS1	Deletion
9q22.2	SHC3, SYK	Deletion
9q22.32–22.33	FANCC, PTCH1	Deletion
10p15.1–14	KLF6, NET1	Deletion
10p13–p12.1	RSU1	Deletion
10q11.21–11.22	NRP1, PARD3, RET	Deletion
10q22.2	ANXA7	Deletion
10q24.1–24.32	SLIT1	Deletion
22q12.3	TIMP3	Deletion

frequent and consistently observed deletions on chromosomes 9q, 10p, 10q and 22q (Table 5). This confirms previous CGH data from thyroid tumours (Kitamura *et al*., 1999; Singh *et al*., 2000; Kadota *et al*., 2003; Finn *et al*., 2004; Richter *et al*., 2004). The similarity in the results from conventional and array CGH demonstrates the reliability of the array CGH approach we used. In addition, we have also validated our array CGH findings for specific chromosomal regions (Tables 3 and 4) by FISH on FFPE sections. In the majority of cases, matching results could be observed by array CGH and FISH.

The PTC cohort investigated in this study consists of sporadic adult and post-Chernobyl tumours, and is characterized by a high frequency of RET/PTC rearrangements and only three sporadic adult cases with BRAF T1796A mutations. This is a surprising finding in sporadic adult PTC because, on the basis of literature, these tumours are expected to exhibit a higher BRAF mutation rate and a lower RET/PTC frequency (Ciampi and Nikiforov, 2007). This contradicting result can be

explained by the RET/PTC enriched selection of sporadic tumours, which subsequently caused an under-representation of BRAF mutations in the sporadic cases, as RET/PTC and BRAF mutations rarely occur simultaneously (Ciampi and Nikiforov, 2007). We specifically chose a cohort with such features to generate data with a homogeneous genetic background, while a mixture of cases with RET/PTC and BRAF mutations would have weakened the statistical power in terms of grouping, especially the RET/PTC-negative cases together.

Our array CGH data and following cluster analysis clearly show a discrimination of nine cases from all other cases and, thus, reflects a different genomic aberration pattern in PTC from adults without RET/PTC rearrangement in comparison to PTC with RET/PTC rearrangements. This finding led us to separate our PTC cases according to their RET/PTC status and age. It is of note that a statistical comparison of RET/PTC-positive cases from adults, RET/PTC-positive cases from children aged under 16 years at operation and RET/PTC-negative cases from adults revealed specific aberration signatures for particular tumour groups (Table 2), while sharing other deletions/gains in chromosomal regions. We have clearly demonstrated that RET/PTC-positive and RET/PTC-negative PTC show different chromosomal aberration patterns.

Losses on chromosome 1p35–36 discriminated between adult and childhood RET/PTC-positive PTC, whereas losses on chromosome 7 appear to be specific for adult RET/PTC-negative cases, and aberrations on chromosome 1p, 3q, 4p, 7p, 9p/q, 10q, 12q, 13q and 21q differentiate between adult and childhood PTCs. The detailed list of characteristic aberrations in RET/PTC-positive and RET/PTC-negative PTCs (Table 2) provided a starting point for mining candidate genes from databases in altered regions that are located within the BAC clones from the array. This analysis revealed 31 candidate genes that have already been reported to be related to tumour growth and development (Table 4). In addition to these specific classifiers in PTC, which are dependent on RET/PTC status and age, we identified 15 tumour-related candidate genes (Table 5) that occur consistently in each tumour and independently of these parameters. It is of note that 21 tumour-suppressor genes map within either the specific or the consistently altered regions. TIMP3 and PTEN have already been reported as tumour suppressors in thyroid tumours (Hu *et al*., 2006; Hou *et al*., 2007; Wang *et al*., 2007), while others are involved in a variety of different tumour types, for example, TGFBR3 and ANXA7 in prostate cancer (Torosyan *et al*., 2006; Dong *et al*., 2007), TNFSF15 and TUSC1 in lung cancer (Shan *et al*., 2004; Hou *et al*., 2005), SYK and Net1 in breast cancer (Repana *et al*., 2006; Huang *et al*., 2007), SLIT1, RSU1 and KLF6 in gliomas and glioblastosmas (Chunduru *et al*., 2002; Dickinson *et al*., 2004; Camacho-Vanegas *et al*., 2007), DBC1 in bladder cancer (Louhelainen *et al*., 2006), DEC1 in oesophageal squamous cell carcinomas (Yang *et al*., 2005), RB1 in retinoblastoma (Corson and Gallie, 2007) and LATS2 and DLEU7 in leukaemias (Hammarsund *et al*., 2004; Jimenez-Velasco *et al*., 2005). Some of these tumour suppressors have influence on the regulation of chromatin acetylation (ING1: Doyon *et al*., 2006), on genome instability (RMI1: Chang *et al*., 2005), on cell cycle progression (PTCH1: Adolphe *et al*., 2006) and on the PI3K/Akt signalling pathway and growth of cancers (PTEN: Wang *et al*., 2007 and PPP1R2: Takakura *et al*., 2001). In contrast, there are also proto-oncogenes affected by these chromosomal changes, for example, JAK1, TFRG, RHOH, TIAM1, ERG, PXN, RNF34, which are overexpressed in many tumours (Azuma *et al*., 2005; Engers *et al*., 2006; Konishi *et al*., 2006; O'Donnell *et al*., 2006; Demichelis *et al*., 2007; Duquette *et al*., 2007). Of special interest are candidate genes that are known to interact with either the MAP kinase pathway or directly with the RET proto-oncogene. These are either involved in RAS signalling (STX17: Zhang *et al*., 2005; RSU1: Chunduru *et al*., 2002), are induced by RET/PTC (JAK2: Puxeddu *et al*., 2005) or are a substrate of RET in thyroid tumours (SHC3: De Falco *et al*., 2005).

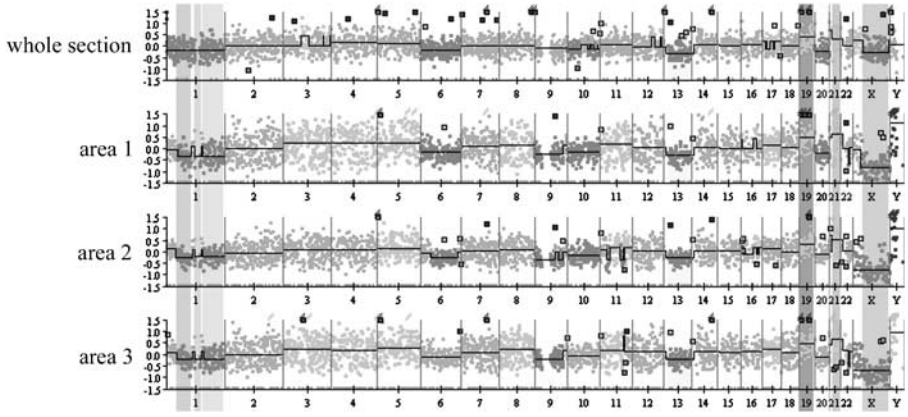

Figure 5 Whole genome array comparative genomic hybridization (CGH) profiles of case no. 3. Grey dots represent bacterial artificial chromosome (BAC) clones within normal regions, red dots indicate BAC clones within deleted and green dots indicate BAC clones within amplified chromosomal regions. Dots within a small black square are BAC clones representing statistical outliers. The profile on the top depicts a whole tumour profile of case no. 3. The profiles below originate from different microdissected areas of the same case. Recurrent chromosomal imbalances between all profiles are indicated by vertical bars.

Another interesting gene affected by a deletion is FANCC, which is known to be downregulated in head and neck cancers (Wreesmann *et al*., 2007) and is part of the Fanconi's anaemia/BRCA pathway, which is frequently disrupted in tumours with poor prognosis. Two genes of the apoptosis pathway, TNFRSF25 and CASP9, are located within the deleted region on 1p35.3–36.31, which is specific for RET/PTC-positive cases from adults. TNFRSF25 is also a candidate tumour suppressor in neuroblastomas (Okawa *et al*., 2008), whereas CASP9 deregulation has frequently been described in human cancers, for example in gastric carcinomas where it is reported that its activation is inhibited by phosphorylation through the MAP kinase pathway (Yoo *et al*., 2007). An interesting finding of this study is the deletion of RET because its activated form, RET/PTC, is known as a marker of PTC. This apparent contradiction, being simultaneously present as an activated oncogene and affected by a deletion, can be explained by a distinct genetic heterogeneity in tumour tissues as already extensively reported for RET/PTC (Unger *et al*., 2004, 2006; Ciampi and Nikiforov, 2007). We confirmed this genetic heterogeneity for RET/PTC by performing RET/PTC analysis at a single-cell level by FISH in this study (data not shown). Thus, it appears that within one tumour, RET/PTC is present in a subgroup of tumour cells, while RET is obviously deleted in another tumour cell population. Interestingly, a distinct heterogeneous distribution of gene alterations within a tumour became apparent also for deletions and amplifications confirmed by FISH with BAC clones for selected regions (Figure 4) and by array CGH analysis of three microdissected areas of RET/PTC-positive tumour case no. 3. From the latter experiment it became obvious that some alterations are recurrent in each area and, thus, visible in the whole tumour profile, but in contrast, numerous imbalances are present only in subgroups of tumour cells. This is also the case for deletions on chromosome 10 involving the RET locus, which appeared deleted in two microdissected areas, but not deleted in another area resulting in a profile for the whole tumour where chromosome 10 deletion is only marginally visible.

To define molecular pathways involving the identified candidate genes, we used the web-accessible Pathway Interaction Database. It turned out that the apoptosis, interleukin-27, angiopoietin receptor and the PI3K/MAP kinase pathways are related to these candidate genes. The well-known tumour-suppressor gene, RB1, which was deleted in the RET/PTC-positive group of tumours and which is a key gene in the FAS signalling pathway (Nagata, 1994) is linked to the caspase cascade in the apoptosis pathway by CASP3 (Riedl and Salvesen, 2007). In normal cells an activation of RB1 by CASP3 leads to a repressed transcription of a series of cell cycle proteins by recruiting methyl-transferases that subsequently induce transcription-inactive heterochromatin (Tan and Wang, 1998; Nielsen *et al*., 2001). A lack of this process RB1-deleted tumour cells may lead to increased genomic instability and tumour progression.

The protein tumour necrosis factor-α, which is upstream of the caspase cascade of the apoptosis pathway and which appeared deleted in the RET/PTC-positive tumour group, connects this pathway to the interleukin-27-mediated pathway (JAK1/2, tyrosine kinase, deleted in the RET/PTC-positive tumour group), to the angiopoietin receptor pathway (FOXO1A, transcription factor, deleted in the RET/PTC-positive tumour group) and to the PI3K pathway. The latter pathway is also related to TIAM1, which is amplified in the RET/PTC-positive tumour group. A central protein of this pathway, RAC, is usually activated by TIAM1 or by PI3K (Collard *et al*., 1996; Worthylake *et al*., 2000; Djeu *et al*., 2002) and acts as a negative regulator. Another protein with the same function in the PI3K pathway is the tumour supressor gene PTEN (Li and Ross, 2007), which was found to be deleted in the RET/PTC-positive tumours of our study.

In conclusion, our findings indicate that different routes of tumour development in PTC are likely to exist. There are additional alterations in RET/PTC-positive tumours, which may act as modifiers of RET activation. This is supported by the finding that the MAP kinase pathway appeared to be linked to a network of pathways of which the apoptosis and the PI3K pathways are most prominent. The involvement of different pathways is also in line with the finding of genetic heterogeneity within PTC from this and previous studies. Different characteristic alterations in RET/PTC-negative tumours indicate alternative paths of tumour development. These would appear to be different from aberrations that may relate to BRAF mutation, as we were unable to detect BRAF mutation in a significant number of sporadic tumours using a previously validated technique (Powell *et al*., 2005). The data presented here may serve as a starting point for further expression and functional studies of the reported candidate genes and point to a very complex nature of genetic alterations in PTC.

Materials and methods

Patient data, treatment and tumour tissues

Tumour samples were collected from 33 patients with PTC. Twenty of these were adults at the time of clinical presentation (16 female, 4 male) and were operated at the Thyroid Tumour Centre in Minsk, Belarus. In addition, 13 childhood patients (eight female, five male) with histologically verified PTCs, developed in the aftermath of the Chernobyl reactor accident, were obtained from the Institute of Endocrinology and Metabolism in Kiev, Ukraine. Appropriate informed consent was obtained from the patients or their guardians. The study was approved by the Ethics Committee of the Bavarian General Medical Council. All tumours were diagnosed as papillary carcinomas, according to the WHO classification of thyroid tumours (DeLellis *et al*., 2004) and further subdivided according to their dominant histological architecture (papillary, follicular, solid). All childhood PTC cases showed a dominantly solid phenotype. Patient data are summarized in Table 1. A tissue section adjacent to that used for DNA extraction was stained with haematoxylin and eosin,

and the presence of tumour epithelium was verified. Slides for DNA extraction and subsequent FISH studies were obtained by microdissection of areas of normal tissue from the slide, resulting in tumour cell enrichment. Either FFPE sections or frozen tissue sections were used for DNA isolation for array CGH. FISH experiments were performed on FFPE sections.

Intratumour heterogeneity of RET/PTC-positive case no. 3
From PTC case no. 3 (Table 1) three histologically similar areas have been isolated by microdissection for further DNA isolation and array CGH analysis. The isolated DNA was amplified by whole genome amplification using the GenomePlex Complete Whole Genome Amplification Kit (Sigma, Taufkirchen, Germany) according to the manufacturer's instructions before array CGH. We exemplarily studied the genetic heterogeneity in PTC, with regard to copy number alterations, by comparing the array CGH profiles of the microdissected areas with that obtained from the whole tumour.

Array CGH
To detect small imbalances beyond the spatial resolution of chromosomal CGH, we performed array CGH analyses of PTCs from 33 patients (Table 1). BAC array slides (1 Mb) containing approximately 3400 BAC clones covering the whole human genome in 1-Mb distances (Fiegler *et al*., 2003) were spotted in duplicates onto amino-reactive slides (CodeLink, GE Healthcare, Buckinghamshire, England).

To ensure that the extracted DNA was of required quality for use in array CGH experiments, a gene-specific multiplex PCR was used (van Beers *et al*., 2006). Only cases with amplification products larger or equal than 300 bp were designated to be of sufficient quality for array CGH analysis. For each experiment, 450 ng of either female or male reference DNA (Promega, Mannheim, Germany) and 450 ng tumour DNA were labelled with Cy3-dCTP and Cy5-dCTP (Perkin Elmer, Shelton, USA), respectively, in an overnight incubation at 37 °C using the BioPrime-Labelling Kit (Invitrogen, Karlsruhe, Germany). Test and reference DNAs were co-hybridized for 40 h with 135 μg cot-1 DNA (Invitrogen), washed and dried in an automated hybridization station (HS400, Tecan, Crailsheim, Germany). Hybridizations have been performed 'sex-mismatched', which means that male tumour DNA was hybridized versus female reference DNA and vice versa. The slides were scanned (GenePix Personal 4100A, Axon Laboratories, Molecular Devices Corp, Chicago, IL, USA) and intensity ratios measured with an array-analysis software (GenePix Pro 6.0, Axon Laboratories). Further data analysis was performed using the web-based array CGH evaluation platform CAPweb (Hupe *et al*., 2004; Neuvial *et al*., 2006), which was installed on a local via an intranet accessible web server. After import of raw data into CAPweb, the normalization procedure using the R-package MANOR was performed using default parameters (exclusion of data points with a replicate deviation of >0.1 and/or a foreground to background signal ratio of <3). Segmentation of the data set using the R-package GLAD, which is connected to CAPweb was performed using default parameters with exception of the parameters GLAD.deltaN (set to 1 times the standard deviation (s.d.) of smoothed Log2 ratios of each data set) and GLAD. forceGL1/2 (set to 1.2 times s.d. of smoothed Log2 ratios of each data set). Data were exported to the array data visualization tool VAMP (La Rosa *et al*., 2006) and analysed for genomic copy number alterations. Common regions of alterations of the analysed cases were determined using the minimal-alteration algorithm (Rouveirol *et al*., 2006), which is integrated into the VAMP software. Regions representing copy number alterations were further analysed using the web-accessible database Ensembl (http://www.ensembl.org) on the basis of NCBI build 36.

FISH analysis using BAC clones
We selected BAC clones from the 1 Mb BAC array, representing amplified or deleted regions (1p22, 1q31, 3p12, 6q21, 7p22, 12q24, 13q21, 19q13, 20q13) and labelled BAC-DNA with biotin or digoxigenin by nick translation according to the standard protocols. Hybridization of BAC clones to paraffin-embedded tissue sections of a representative PTC case carrying the respective alteration and detection of fluorescent signals were performed as described previously (Unger *et al*., 2004).

BRAF T1796 mutation analysis
The frequency of the BRAF T1796 mutation was investigated by PCR as published previously (Powell *et al*., 2005). Briefly, PCR was used to amplify a 224 bp sequence in exon 15 of the BRAF gene using forward primer 5′-TCATAATGCTTGC TCTGATAGGA-3′ and reverse primer 5′-GGCCAAAAATT TAATCAGTGGA-3′. Reactions contained 2.5 mM $MgCl_2$, 0.2 mM dNTPs, 1 μM of each primer and 0.5 U of AmpliTaq Gold polymerase (Applied Biosystems, Warrington, UK) in a total volume of 30 μl. Five microliters of each PCR product were run on a 2% agarose gel to assess size and amount of amplification products. The 224 bp amplimer was further cut with TspR1. In the mutated sequence, one TspR1 site is lost leading to different digestion products. Five microliters of each PCR product were digested, and restriction fragments were resolved on polyacrylamide gels with silver staining.

Statistical analysis
Distinct genome-wide patterns of chromosomal imbalances were explored using (i) unsupervised HCA on the basis of correlation coefficient distance and average linkage method; (ii) principal component analysis. Fisher's exact test was then used for association of groups from cluster analysis with those given by patient characteristics (age status, RET/PTC status), and for statistical two-group comparisons of amplified and deleted regions. Every BAC clone within altered regions was tested. If the alteration occurred at least five times within a tumour group, *P*-values have been adjusted using the Benjamini–Hochberg FDR-controlling procedure to obtain reliable significance levels with the high number of tests performed. Results of statistical tests were assigned to chromosomal segments for a clear presentation of data (shown in Table 2).

Abbreviations

BAC, bacterial artificial chromosome; CGH, comparative genomic hybridization; FISH, fluorescence *in situ* hybridization; PTC, papillary thyroid carcinoma.

Acknowledgements

We acknowledge Elke Konhäuser for the skilful technical assistance and Cordelia Langford and the Wellcome Trust Sanger Institute microarray facility for supplying the 1-Mb BAC arrays. This study was supported in part by EC Grant FP6-36495 and a grant from the German Cancer Aid (project no. 108033).

References

Adolphe C, Hetherington R, Ellis T, Wainwright B. (2006). Patched1 functions as a gatekeeper by promoting cell cycle progression. *Cancer Res* **66**: 2081–2088.

Azuma K, Tanaka M, Uekita T, Inoue S, Yokota J, Ouchi Y *et al*. (2005). Tyrosine phosphorylation of paxillin affects the metastatic potential of human osteosarcoma. *Oncogene* **24**: 4754–4764.

Camacho-Vanegas O, Narla G, Teixeira MS, DiFeo A, Misra A, Singh G *et al*. (2007). Functional inactivation of the KLF6 tumor suppressor gene by loss of heterozygosity and increased alternative splicing in glioblastoma. *Int J Cancer* **121**: 1390–1395.

Chang M, Bellaoui M, Zhang C, Desai R, Morozov P, Delgado-Cruzata L *et al*. (2005). RMI1/NCE4, a suppressor of genome instability, encodes a member of the RecQ helicase/Topo III complex. *EMBO J* **24**: 2024–2033.

Cheung CC, Ezzat S, Ramyar L, Freeman JL, Asa SL. (2000). Molecular basis off hurthle cell papillary thyroid carcinoma. *J Clin Endocrinol Metab* **85**: 878–882.

Chunduru S, Kawami H, Gullick R, Monacci WJ, Dougherty G, Cutler ML. (2002). Identification of an alternatively spliced RNA for the Ras suppressor RSU-1 in human gliomas. *J Neurooncol* **60**: 201–211.

Ciampi R, Nikiforov YE. (2007). RET/PTC rearrangements and BRAF mutations in thyroid tumorigenesis. *Endocrinology* **148**: 936–941.

Collard JG, Habets GG, Michiels F, Stam J, van der Kammen RA, van Leeuwen F. (1996). Role of Tiam 1 in Rac-mediated signal transduction pathways. *Curr Top Microbiol Immunol* **213**(Part 2): 253–265.

Corson TW, Gallie BL. (2007). One hit, two hits, three hits, more? Genomic changes in the development of retinoblastoma. *Genes Chromosomes Cancer* **46**: 617–634.

De Falco V, Guarino V, Malorni L, Cirafici AM, Troglio F, Erreni M *et al*. (2005). RAI(ShcC/N-Shc)-dependent recruitment of GAB 1 to RET oncoproteins potentiates PI 3-K signalling in thyroid tumors. *Oncogene* **24**: 6303–6313.

DeLellis RA, Lloyd RV, Heitz PU, Eng C (eds) (2004). *World Health Organization Classification of Tumours, Pathology and Genetics of Tumours of Endocrine Organs*. IARC Press: Lyon.

Demichelis F, Fall K, Perner S, Andren O, Schmidt F, Setlur SR *et al*. (2007). TMPRSS2:ERG gene fusion associated with lethal prostate cancer in a watchful waiting cohort. *Oncogene* **26**: 4596–4599.

Dickinson RE, Dallol A, Bieche I, Krex D, Morton D, Maher ER *et al*. (2004). Epigenetic inactivation of SLIT3 and SLIT1 genes in human cancers. *Br J Cancer* **91**: 2071–2078.

Djeu JY, Jiang K, Wei S. (2002). A view to a kill: signals triggering cytotoxicity. *Clin Cancer Res* **8**: 636–640.

Dong M, How T, Kirkbride KC, Gordon KJ, Lee JD, Hempel N *et al*. (2007). The type III TGF-beta receptor suppresses breast cancer progression. *J Clin Invest* **117**: 206–217.

Doyon Y, Cayrou C, Ullah M, Landry AJ, Cote V, Selleck W *et al*. (2006). ING tumor suppressor proteins are critical regulators of chromatin acetylation required for genome expression and perpetuation. *Mol Cell* **21**: 51–64.

Duquette ML, Huber MD, Maizels N. (2007). G-rich proto-oncogenes are targeted for genomic instability in B-cell lymphomas. *Cancer Res* **67**: 2586–2594.

Elisei R, Romei C, Vorontsova T, Cosci B, Veremeychik V, Kuchinskaya E *et al*. (2001). RET/PTC rearrangements in thyroid nodules: studies in irradiated and not irradiated, malignant and benign thyroid lesions in children and adults. *J Clin Endocrinol Metab* **86**: 3211–3216.

Engers R, Mueller M, Walter A, Collard JG, Willers R, Gabbert HE. (2006). Prognostic relevance of Tiam1 protein expression in prostate carcinomas. *Br J Cancer* **95**: 1081–1086.

Fiegler H, Carr P, Douglas EJ, Burford DC, Hunt S, Scott CE *et al*. (2003). DNA microarrays for comparative genomic hybridization based on DOP-PCR amplification of BAC and PAC clones. *Genes Chromosomes Cancer* **36**: 361–374.

Finn SP, Smyth P, O'Regan E, Cahill S, Flavin R, O'Leary J *et al*. (2004). Array comparative genomic hybridisation analysis of gamma-irradiated human thyrocytes. *Virchows Arch* **445**: 396–404.

Grieco M, Santoro M, Berlingieri MT, Melillo RM, Donghi R, Bongarzone I *et al*. (1990). PTC is a novel rearranged form of the ret proto-oncogene and is frequently detected *in vivo* in human thyroid papillary carcinomas. *Cell* **60**: 557–563.

Hammarsund M, Corcoran MM, Wilson W, Zhu C, Einhorn S, Sangfelt O *et al*. (2004). Characterization of a novel B-CLL candidate gene—DLEU7—located in the 13q14 tumor suppressor locus. *FEBS Lett* **556**: 75–80.

Hou P, Liu D, Shan Y, Hu S, Studeman K, Condouris S *et al*. (2007). Genetic alterations and their relationship in the phosphatidylinositol 3-kinase/Akt pathway in thyroid cancer. *Clin Cancer Res* **13**: 1161–1170.

Hou W, Medynski D, Wu S, Lin X, Li LY. (2005). VEGI-192, a new isoform of TNFSF15, specifically eliminates tumor vascular endothelial cells and suppresses tumor growth. *Clin Cancer Res* **11**: 5595–5602.

Hu S, Liu D, Tufano RP, Carson KA, Rosenbaum E, Cohen Y *et al*. (2006). Association of aberrant methylation of tumor suppressor genes with tumor aggressiveness and BRAF mutation in papillary thyroid cancer. *Int J Cancer* **119**: 2322–2329.

Huang H, Sossey-Alaoui K, Beachy SH, Geradts J. (2007). The tetraspanin superfamily member NET-6 is a new tumor suppressor gene. *J Cancer Res Clin Oncol* **133**: 761–769.

Hupe P, Stransky N, Thiery JP, Radvanyi F, Barillot E. (2004). Analysis of array CGH data: from signal ratio to gain and loss of DNA regions. *Bioinformatics* **20**: 3413–3422.

Ishizaka Y, Kobayashi S, Ushijima T, Hirohashi S, Sugimura T, Nagao M. (1991). Detection of retTPC/PTC transcripts in thyroid adenomas and adenomatous goiter by an RT-PCR method. *Oncogene* **6**: 1667–1672.

Jhiang SM, Mazzaferri EL. (1994). The ret/PTC oncogene in papillary thyroid carcinoma. *J Lab Clin Med* **123**: 331–337.

Jimenez-Velasco A, Roman-Gomez J, Agirre X, Barrios M, Navarro G, Vazquez I *et al*. (2005). Downregulation of the large tumor suppressor 2 (LATS2/KPM) gene is associated with poor prognosis in acute lymphoblastic leukemia. *Leukemia* **19**: 2347–2350.

Kadota M, Tamaki Y, Sekimoto M, Fujiwara Y, Aritake N, Hasegawa S *et al*. (2003). Loss of heterozygosity on chromosome 16p and 18q in anaplastic thyroid carcinoma. *Oncol Rep* **10**: 35–38.

Kitamura Y, Shimizu K, Nagahama M, Sugino K, Ozaki O, Mimura T *et al*. (1999). Immediate causes of death in thyroid carcinoma: clinicopathological analysis of 161 fatal cases. *J Clin Endocrinol Metab* **84**: 4043–4049.

Klugbauer S, Lengfelder E, Demidchik EP, Rabes HM. (1995). High prevalence of RET rearrangement in thyroid tumors of children from Belarus after the Chernobyl reactor accident. *Oncogene* **11**: 2459–2467.

Konishi T, Sasaki S, Watanabe T, Kitayama J, Nagawa H. (2006). Overexpression of hRFI inhibits 5-fluorouracil-induced apoptosis in colorectal cancer cells via activation of NF-kappaB and upregulation of BCL-2 and BCL-XL. *Oncogene* **25**: 3160–3169.

La Rosa P, Viara E, Hupe P, Pierron G, Liva S, Neuvial P *et al*. (2006). VAMP: visualization and analysis of array-CGH, transcriptome and other molecular profiles. *Bioinformatics* **22**: 2066–2073.

Li L, Ross AH. (2007). Why is PTEN an important tumor suppressor? *J Cell Biochem* **102**: 1368–1374.

Louhelainen JP, Hurst CD, Pitt E, Nishiyama H, Pickett HA, Knowles MA. (2006). DBC1 re-expression alters the expression of multiple components of the plasminogen pathway. *Oncogene* **25**: 2409–2419.

Nagata S. (1994). Fas and Fas ligand: a death factor and its receptor. *Adv Immunol* **57**: 129–144.

Neuvial P, Hupe P, Brito I, Liva S, Manie E, Brennetot C *et al*. (2006). Spatial normalization of array-CGH data. *BMC Bioinformatics* **7**: 264.

Nielsen SJ, Schneider R, Bauer UM, Bannister AJ, Morrison A, O'Carroll D *et al*. (2001). Rb targets histone H3 methylation and HP1 to promoters. *Nature* **412**: 561–565.

O'Donnell KA, Yu D, Zeller KI, Kim JW, Racke F, Thomas-Tikhonenko A *et al*. (2006). Activation of transferrin receptor 1 by c-Myc enhances cellular proliferation and tumorigenesis. *Mol Cell Biol* **26**: 2373–2386.

Okawa ER, Gotoh T, Manne J, Igarashi J, Fujita T, Silverman KA *et al*. (2008). Expression and sequence analysis of candidates for the 1p36.31 tumor suppressor gene deleted in neuroblastomas. *Oncogene* **27**: 803–810.

Pierotti MA, Santoro M, Jenkins RB, Sozzi G, Bongarzone I, Grieco M *et al*. (1992). Characterization of an inversion on the long arm of chromosome 10 juxtaposing D10S170 and RET and creating the oncogenic sequence RET/PTC. *Proc Natl Acad Sci USA* **89**: 1616–1620.

Powell N, Jeremiah S, Morishita M, Dudley E, Bethel J, Bogdanova T *et al*. (2005). Frequency of BRAF T1796A mutation in papillary thyroid carcinoma relates to age of patient at diagnosis and not to radiation exposure. *J Pathol* **205**: 558–564.

Puxeddu E, Knauf JA, Sartor MA, Mitsutake N, Smith EP, Medvedovic M *et al*. (2005). RET/PTC-induced gene expression in thyroid PCCL3 cells reveals early activation of genes involved in regulation of the immune response. *Endocr Relat Cancer* **12**: 319–334.

Rabes HM, Demidchik EP, Sidorow JD, Lengfelder E, Beimfohr C, Hoelzel D *et al*. (2000). Pattern of radiation-induced RET and NTRK1 rearrangements in 191 post-chernobyl papillary thyroid carcinomas: biological, phenotypic, and clinical implications. *Clin Cancer Res* **6**: 1093–1103.

Repana K, Papazisis K, Foukas P, Valeri R, Kortsaris A, Deligiorgi E *et al*. (2006). Expression of Syk in invasive breast cancer: correlation to proliferation and invasiveness. *Anticancer Res* **26**: 4949–4954.

Rhoden KJ, Johnson C, Brandao G, Howe JG, Smith BR, Tallini G. (2004). Real-time quantitative RT-PCR identifies distinct c-RET, RET/PTC1 and RET/PTC3 expression patterns in papillary thyroid carcinoma. *Lab Invest* **84**: 1557–1570.

Rhoden KJ, Unger K, Salvatore G, Yilmaz Y, Vovk V, Chiappetta G *et al*. (2006). RET/papillary thyroid cancer rearrangement in nonneoplastic thyrocytes: follicular cells of Hashimoto's thyroiditis share low-level recombination events with a subset of papillary carcinoma. *J Clin Endocrinol Metab* **91**: 2414–2423.

Richter H, Braselmann H, Hieber L, Thomas G, Bogdanova T, Tronko N *et al*. (2004). Chromosomal imbalances in post-chernobyl thyroid tumors. *Thyroid* **14**: 1061–1064.

Riedl SJ, Salvesen GS. (2007). The apoptosome: signalling platform of cell death. *Nat Rev Mol Cell Biol* **8**: 405–413.

Rouveirol C, Stransky N, Hupe P, Rosa PL, Viara E, Barillot E *et al*. (2006). Computation of recurrent minimal genomic alterations from array-CGH data. *Bioinformatics* **22**: 849–856.

Santoro M, Carlomagno F, Melillo RM, Fusco A. (2004). Dysfunction of the RET receptor in human cancer. *Cell Mol Life Sci* **61**: 2954–2964.

Shan Z, Parker T, Wiest JS. (2004). Identifying novel homozygous deletions by microsatellite analysis and characterization of tumor suppressor candidate 1 gene, TUSC1, on chromosome 9p in human lung cancer. *Oncogene* **23**: 6612–6620.

Singh B, Lim D, Cigudosa JC, Ghossein R, Shaha AR, Poluri A *et al*. (2000). Screening for genetic aberrations in papillary thyroid cancer by using comparative genomic hybridization. *Surgery* **128**: 888–893; discussion 893–894.

Smida J, Salassidis K, Hieber L, Zitzelsberger H, Kellerer AM, Demidchik EP *et al*. (1999). Distinct frequency of ret rearrangements in papillary thyroid carcinomas of children and adults from Belarus. *Int J Cancer* **80**: 32–38.

Takakura S, Kohno T, Manda R, Okamoto A, Tanaka T, Yokota J. (2001). Genetic alterations and expression of the protein phosphatase 1 genes in human cancers. *Int J Oncol* **18**: 817–824.

Tan X, Wang JY. (1998). The caspase-RB connection in cell death. *Trends Cell Biol* **8**: 116–120.

Thomas GA, Bunnell H, Cook HA, Williams ED, Nerovnya A, Cherstvoy ED *et al*. (1999). High prevalence of RET/PTC rearrangements in Ukrainian and Belarussian post-Chernobyl thyroid papillary carcinomas: a strong correlation between RET/PTC3 and the solid-follicular variant. *J Clin Endocrinol Metab* **84**: 4232–4238.

Torosyan Y, Dobi A, Naga S, Mezhevaya K, Glasman M, Norris C *et al*. (2006). Distinct effects of annexin A7 and p53 on arachidonate lipoxygenation in prostate cancer cells involve 5-lipoxygenase transcription. *Cancer Res* **66**: 9609–9616.

Unger K, Zitzelsberger H, Salvatore G, Santoro M, Bogdanova T, Braselmann H *et al*. (2004). Heterogeneity in the distribution of RET/PTC rearrangements within individual post-Chernobyl papillary thyroid carcinomas. *J Clin Endocrinol Metab* **89**: 4272–4279.

Unger K, Zurnadzhy L, Walch A, Mall M, Bogdanova T, Braselmann H *et al*. (2006). RET rearrangements in post-Chernobyl papillary thyroid carcinomas with a short latency analysed by interphase FISH. *Br J Cancer* **94**: 1472–1477.

van Beers EH, Joosse SA, Ligtenberg MJ, Fles R, Hogervorst FB, Verhoef S *et al*. (2006). A multiplex PCR predictor for aCGH success of FFPE samples. *Br J Cancer* **94**: 333–337.

Wang Y, Hou P, Yu H, Wang W, Ji M, Zhao S *et al*. (2007). High prevalence and mutual exclusivity of genetic alterations in the phosphatidylinositol-3-kinase/akt pathway in thyroid tumors. *J Clin Endocrinol Metab* **92**: 2387–2390.

Worthylake DK, Rossman KL, Sondek J. (2000). Crystal structure of Rac1 in complex with the guanine nucleotide exchange region of Tiam1. *Nature* **408**: 682–688.

Wreesmann VB, Estilo C, Eisele DW, Singh B, Wang SJ. (2007). Downregulation of Fanconi anemia genes in sporadic head and neck squamous cell carcinoma. *ORL J Otorhinolaryngol Relat Spec* **69**: 218–225.

Yang L, Leung AC, Ko JM, Lo PH, Tang JC, Srivastava G *et al*. (2005). Tumor suppressive role of a 2.4 Mb 9q33–q34 critical region and DEC1 in esophageal squamous cell carcinoma. *Oncogene* **24**: 697–705.

Yoo NJ, Lee SH, Jeong EG. (2007). Expression of phosphorylated caspase-9 in gastric carcinomas. *APMIS* **115**: 354–359.

Zhang Q, Li J, Deavers M, Abbruzzese JL, Ho L. (2005). The subcellular localization of syntaxin 17 varies among different cell types and is altered in some malignant cells. *J Histochem Cytochem* **53**: 1371–1382.

Supplementary Information accompanies the paper on the Oncogene website (http://www.nature.com/onc).